



Improving early warning of drought-driven food insecurity in Southern Africa using operational hydrological monitoring and forecasting products

Shraddhanand Shukla¹, Kristi R. Arsenault^{2,3}, Abheera Hazra^{4,3}, Christa Peters-Lidard³, Randal D. Koster³, Frank Davenport¹, Tamuka Magadzire^{5,1}, Chris Funk^{6,1}, Sujay Kumar³, Amy McNally^{2,5}, Augusto Getirana^{4,3}, Greg Husak¹, Ben Zaitchik⁷, Jim Verdin^{8,5}, Faka Dieudonne Nsadisa⁹, Inbal Becker-Reshef^{3,4}

¹University of California, Santa Barbara, California, USA

²SAIC, Reston, Virginia, USA

³NASA Goddard Space Flight Center, Greenbelt, Maryland, USA

⁴University of Maryland, Maryland, USA

⁵Famine Early Warning Systems Network, Washington D.C., USA

⁶EROS, United States Geological Survey, Sioux Falls, South Dakota, USA

⁷John Hopkins University, Baltimore, Maryland, USA

⁸United States Agency for International Development, Washington D.C., USA

⁹Southern African Development Community Climate Services Center, Botswana

Correspondence to: Shraddhanand Shukla (sshukla@ucsb.edu)

1 **Abstract:** The region of southern Africa (SA) has a fragile food economy and is vulnerable to
2 frequent droughts. In 2015-2016, an El Niño-driven drought resulted in major maize production
3 shortfalls, food price increases, and livelihood disruptions that pushed 29 million people into



4 severe food insecurity. Interventions to mitigate food insecurity impacts require early warning of
5 droughts —preferably as early as possible before the harvest season (typically, starting in April)
6 and lean season (typically, starting in November). Hydrologic monitoring and forecasting
7 systems provide a unique opportunity to support early warning efforts, since they can provide
8 regular updates on available rootzone soil moisture (RZSM), a critical variable for crop yield,
9 and provide forecasts of RZSM by combining the estimates of antecedent soil moisture
10 conditions with climate forecasts. For SA, this study documents the predictive capabilities of a
11 recently developed NASA Hydrological Forecasting and Analysis System (NH_yFAS). The
12 NH_yFAS system’s ability to forecast and monitor the 2015/16 drought event is evaluated. The
13 system’s capacity to explain interannual variations in regional crop yield and identify
14 below-normal crop yield events is also evaluated. Results show that the NH_yFAS products
15 would have identified the regional severe drought event, which peaked during
16 December-February of 2015/2016, at least as early as November 1, 2015. Next, it is shown that
17 February RZSM forecasts produced as early as November 1 (4-5 months before the start of
18 harvest and about a year before the start of the next lean season) correlate fairly well with
19 regional crop yields ($r=0.49$). The February RZSM monitoring product, available in early March,
20 correlates with the regional crop yield with higher skill ($r= 0.79$). It is also found that when the
21 February RZSM forecast produced on November 1 is indicated to be in the lowest tercile, the
22 detrended regional crop yield is below normal about two-thirds (significance level ~86%) of the
23 time. Furthermore, when the February RZSM monitoring product (available in early March)
24 indicates a lowest tercile value, the crop yield is always below normal, at least over the sample



25 years considered. These results indicate that the NHyFAS products can effectively support food
26 insecurity early warning in the SA region.

1 Introduction

27 Southern Africa (SA) is vulnerable to food insecurity. Climate stressors (e.g. precipitation and
28 temperature) are among the important drivers of food insecurity (Misselhorn 2005; Conway et al.
29 2015). The primary rainy season in SA spans October to March, which overlaps the main
30 planting season from October to February (Fig. 1 (a)). This period also covers the lean season,
31 when food supplies are typically limited. April-July is typically the main harvest season, when
32 the food reserve is expected to begin replenishing. In several SA countries, with the Republic of
33 South Africa (RSA) being the main exception, typical monthly variability in food prices closely
34 follows this crop cycle, as shown in Fig. 1(b). The prices typically start to rise after the harvest
35 season and reach their peak just before or near the start of the harvest season. This
36 correspondence between the prices and crop cycles highlights the region's climate-related
37 sensitivity to food insecurity. In the case of below-normal crop yield, the food prices rise even
38 more than normal, reducing access to food for the poorest of the population.

39 The percentage income of wealth shared by the poorest 10% and 20% of the population
40 in several SA countries has not improved significantly over time (not shown here). These
41 portions of the population are likely to be more food insecure in drought years. They already use
42 a relatively higher share of their income on food, and in the case of price rises related to low crop
43 yield, their access to food becomes even more limited.

44 The 2015-16 drought event (attributed to a strong El Niño) in southern Africa further
45 highlighted its vulnerability to climate-related regional food insecurity (Archer et al., 2017; Funk



46 et al., 2018; Pomposi et al., 2018). This event led to a substantial reduction in regional
47 agricultural production—including in the Republic of South Africa (RSA), which is the main
48 crop-producing country in the region—a reduction and rationing of water supplies, a loss of
49 livestock, and an increase in unemployment in the region (SADC, 2016). Throughout the
50 Southern African Development Community (SADC) region in 2015-16, cereal production was
51 down by -10.2% (varying from +61% to -94% in individual member countries) relative to the
52 previous 5-year average (SADC, 2016). Figure 1 (c)-(f) shows a comparison of national retail
53 maize prices (in USD) in several of the SA countries during 2015-16, with the previous 5-year
54 mean prices in those countries. The prices in 2015-16 were substantially higher than the previous
55 5-year mean. Of particular importance is the price increase in RSA, where, typically, the food
56 prices do not vary much throughout the year due to its general self-sufficiency in food
57 production, as well as its international trade. Consumer Price Index (CPI) for food for RSA also
58 experienced a drastic upward shift during the 2015-16 drought year (not shown here). In fact,
59 based on the CPI data (available from the FAO) the CPI was substantially higher than that of the
60 past 5-year mean during the beginning of the following growing season of 2016-17 including in
61 RSA where typically the CPI remains fairly stable during a year. These price shocks can
62 dramatically impact poor households, who typically spend 60% or more of their income on food.
63 According to the recent World Bank Development Indicator, incomes for the poorest 10% and
64 20% of households in these countries have remained generally constant underscoring the depth
65 of poverty (not shown). On average, in Malawi, Mozambique, Zimbabwe and South Africa,
66 these individuals subsist on \$70, \$126, \$288, and \$716 USD a year, respectively.



67 Figure 1(c)-(f) and the income related facts (based on World Bank Development
68 indicator) presented above highlight the severity of food insecurity in a regional drought event
69 like 2015-16. In the 2015-2016 event, food imports from RSA—which is the main producer and
70 exporter of food in the region to the other SA countries—were not enough, and international
71 assistance becomes crucial.

72 This is why in June 2016, the SADC launched a Regional Humanitarian Appeal stating
73 that approximately 40 million people in the region required humanitarian assistance, at a cost of
74 approximately USD \$2.4 billion (Magadzire et al. 2017).

75 Mitigation of the most adverse impacts of food insecurity, like the event of 2015-16,
76 requires timely and effective early warning. An effective early warning system has two key
77 attributes (Funk et al., 2019): (1) the ability to provide routine, frequent early warning of drought
78 status and (2) the ability to incorporate both monitoring and forecasting to best account for the
79 conditions until the date of early warning, in combination with the climate outlook for the
80 upcoming season.

81 A seasonal scale hydrologic forecasting system can potentially effectively support an
82 early warning system, as it can provide updated hydrologic forecasts monthly by accounting for
83 the drought conditions as of the forecast release date and climate outlook over the forecast period
84 (Sheffield et al., 2014; Shukla et al., 2014). However, thus far, the application of seasonal-scale
85 hydrologic forecasts in food insecurity early warning has been limited at best. On the other hand,
86 operational, publicly available, state-of-the-art dynamical climate forecasts have found regular
87 usage in guiding climate outlook, as well as assessments of expected food insecurity. For
88 example, USAID's Famine Early Warning Systems Network (<http://fews.net/>), G20-Group on



89 Earth Observations Global Agricultural Monitoring (GEOGLAM) Crop Monitor for Early
90 Warning, and SADC's Climate Service Center (CSC) all utilize the dynamical climate forecasts
91 as one of their early warning tools. Furthermore, numerous past studies have investigated the
92 predictability of SA climate (Meque and Abiodun, 2014) and examined the skill of diverse
93 approaches in forecasting, particularly of rainfall, as well as streamflow and agricultural
94 production in different parts of this region (Archer et al., 2017; Cane et al., 1994; Diro, 2015;
95 Landman et al., 2001; Landman and Beraki, 2010; Landman and Goddard, 2002; Manatsa et al.,
96 2015; Martin et al., 2000; Sunday et al., 2014; Trambauer et al., 2015; Winsemius et al., 2014).
97 Historically, El Niño-Southern Oscillation (ENSO) has proven to be among the main predictors
98 of this region's climate, with another important predictor being the Southern Indian Ocean
99 Dipole (Hoell et al., 2016, 2017; Hoell and Cheng, 2017).

100 However, the application of climate-model-driven hydrological forecasts, which, as
101 stated above, derive their skills from the climate forecast skill and initial hydrologic conditions,
102 has been limited. Thus, it can be an effective early warning tool, as operational food insecurity
103 assessment has been limited, with the only other main example being the African Flood and
104 Drought Monitor (Sheffield et al., 2014).

105 In August 2018, a new NASA Hydrological Forecasting and Analysis System
106 (NHyFAS), an operational seasonal hydrologic forecasting system (Arsenault et al., 2019), was
107 implemented to support the early warning efforts of FEWS NET, building upon existing
108 hydrologic monitoring (McNally et al., 2017). This study evaluates this system in supporting
109 early warning of regional food insecurity in the SA region. The evaluation is conducted by
110 examining the performance of this system (i) for the 2015-16 drought event, which led to



111 regional food insecurity, (ii) in explaining regional crop yield variability in the region, and (iii) in
112 identifying below normal crop yield events, which are characteristically associated with overall
113 lower food availability in the region and, hence, food insecurity. Regional crop yield is used as a
114 target variable here, as it is among the main contributors to regional food insecurity. It is
115 hypothesized that if this system can skillfully forecast regional crop yield and identify below
116 normal regional crop yields, it can successfully support the early warning of food insecurity in
117 the region.

118 As noted above and shown in Fig. 1(a), April-July is typically the main harvest season,
119 when the food reserve is expected to begin replenishing and last through the lean season, which
120 starts in November. Below-normal food availability during this period can lead to food
121 insecurity. Therefore, early warning systems aim to provide outlooks for food insecurity as far in
122 advance of the harvest and lean season as possible. Consequently, this study focuses on using
123 forecasting and monitoring products that are available in November (4-5 months before the start
124 of the harvest and about a year before the start of the next lean season) through March (1-2
125 months before the start of the harvest and about 8-9 months before the start of the next lean
126 season) to examine their value in supporting early warning of food insecurity in the region.

2 Data and Methodology

2.1 Hydrologic Modeling Framework

127 The hydrologic monitoring and forecasting products used in this study come from the
128 NHyFAS (Arsenault et al., 2019). Arsenault et al. (2019) describes the system in much detail; we
129 provide below a brief description of the products. To generate hydrological forecasts, we use
130 NASA's Catchment land surface model (CLSM; [(Ducharne et al., 2000; Koster et al., 2000) and



131 the Noah Multi-Parameterization (Noah-MP; [Niu et al., 2011; Yang et al., 2011] land surface
132 model (LSM), which account for changes in soil moisture (e.g., root zone) and groundwater
133 storage, and surface energy and water flux terms. These two LSMs are part of the model suite in
134 the Land Information System (LIS) framework (Kumar et al., 2006)—the primary software
135 system used to produce this study’s forecast experiments. Both LSMs were spun-up twice for the
136 period from 1 January, 1981 to 31 December, 2015; then, historical open-loop (OL) runs were
137 generated for January 1981 through 2018. Rootzone SM (RZSM), which is the main hydrologic
138 variable used in this analysis, indicates the soil moisture in the top one meter of the soil profile.
139 The entire depth of the soil profile is different for the two models used in this analysis (typically
140 about 2 m for Noah-MP and about 4 m for CLSM).

2.2 Model Parameters

141 In the version of CLSM used here, hydrologic and catchment parameters (Ducharne et
142 al., 2000) are based on a high-resolution, global topographic data set (Verdin and Verdin, 1999),
143 and soil texture (Reynolds et al., 2000) and profile parameters are derived from the Second
144 Global Soil Wetness Project (GSWP-2; (Guo and Dirmeyer, 2006) data set and mapped to the
145 catchment tiles. Land cover classes are mapped from the University of Maryland AVHRR data
146 set, and vegetation parameters include, for example, leaf area index (LAI), which are also
147 derived from GSWP-2. Albedo scaling factors are based on Moderate Resolution Imaging
148 Spectroradiometer (MODIS) direct and diffuse visible or near infra-red radiation inputs (Moody
149 et al., 2008).

150 Noah-MP vegetation parameters include the modified IGBP MODIS-based land cover
151 data set (Friedl et al., 2002), leaf area index, and monthly greenness fraction (Gutman and



152 Ignatov, 1998). The soil texture data set is based on Reynolds et al. (2000), and soil parameters
153 are mapped to the varying textures. Monthly global (snow-free) albedo (Csiszar and Gutman,
154 1999) and a maximum snow albedo parameter field are also employed. Additional details are
155 found in (Niu et al., 2011).

2.3 Input observed forcings and climate forecasts

156 The spin-up and OL runs used to generate the long-term “observed” climatology of
157 RZSM are driven with NASA’s Modern-Era Retrospective analysis for Research and
158 Applications, version 2 (MERRA-2; [(Gelaro et al., 2017) atmospheric fields (e.g., 2m air
159 temperature, humidity). Precipitation forcing comes from the U.S. Geological Survey
160 (USGS)/University of California, Santa Barbara (UCSB) Climate Hazards Center InfraRed
161 Precipitation with Station data set, version 2.0 (CHIRPSv2; [(Funk et al., 2015).

162 Hindcasts of RZSM are generated by forcing the hydrologic models with NASA’s
163 Goddard Earth Observing System (GEOS) Atmosphere-Ocean General Circulation Model,
164 version 5 (GEOS; [(Borovikov et al., 2017)]) Seasonal-to-Interannual Forecast System. The
165 eleven ensemble members of version 1 of this forecast system that were used in the North
166 American Multi-Model Ensemble (NMME) project are used in the forecast portion of this study.
167 To make the GEOS forecasted meteorology consistent with the meteorology underlying the OL
168 initial conditions, we Bias-Corrected and Spatially Downscaled (BCSD; [(Wood et al., 2002)])
169 the GEOS forecasts using the MERRA-2 and CHIRPS data sets. The BCSD-GEOS forecast files
170 are then ingested into LIS to drive the LSMs and generate the dynamical hydrological forecasts.
171 The BCSD-GEOS hindcasts are initialized on November 1st (near the start of the planting



172 season) and January 1st (middle of the planting season) and are run for each 6-month forecast
173 period from 1982-83 to 2017-18.

174 Hindcasts of RZSM are also generated using the Ensemble Streamflow Prediction (ESP)
175 method (Day 1985; Shukla et al. 2013), where the models are forced with resampled climatology
176 of observed forcings (forcings that are used to drive the OL simulation). The hindcasts generated
177 using the ESP method derive their skills from the initial hydrologic conditions only.

2.4 RZSM Monitoring and forecasting products

178 The performance of the NHyFAS system is evaluated through its RZSM monitoring
179 (generated from OL) and forecasting products. Both products are generated at 0.25 X 0.25
180 degree spatial resolution and daily temporal resolution. Daily values are averaged over a month
181 to get monthly values. The monthly values of the monitoring product are converted to percentiles
182 relative to OL climatology over 1982-2010, and monthly values of the ensemble mean
183 forecasting products (GEOS and ESP based) are converted into percentiles relative to the
184 (ensemble mean) climatology over 1982-2010 of the respective hindcast runs. In both cases,
185 empirical distribution taken from the climatology is considered to convert values to percentiles.
186 Once gridded percentile values are generated they are spatially aggregated over the SA region (as
187 shown in Fig. 2) to get RZSM monitoring and forecasting products over the SA region.

2.5 Regional Crop Yield

188 The regional crop yield is calculated using country-level crop production and area
189 harvested reports. These reports come from the United States Department of Agriculture's
190 Foreign Agricultural Service's Production Supply and Distribution (PSD) database. To compile
191 this database, USDA relies on several sources, including official country statistics, reports from



192 agricultural attaches at U.S. embassies, data from international organizations, publications from
193 individual countries, and information from traders both inside and outside of the target countries.
194 For this study, we focus only on maize, as it is the main crop in the region and the key crop for
195 food security. To get regional crop yield from country-level crop yield, we first converted
196 country-level yield into production using the harvested area (provided by the PSD), added the
197 total production, and then divided it by the sum of the harvested area in all SA countries in our
198 focus domain. The regional crop yield is detrended for the purposes of this study to reduce the
199 effect of any long-term changes (e.g. technological changes) on the crop yield.

3. Results

3.1 Performance of NHyFAS during the 2015-16 drought event

200 As highlighted in section 1, the 2015-16 drought event in SA is among the most severe in
201 terms of drought severity and food insecurity impacts in the last few decades. Therefore, we
202 begin the evaluation of the suitability of NHyFAS in supporting food insecurity early warning in
203 the SA region by examining how this system would have performed during the 2015-16 event.
204 Although the NHyFAS operationally provides the seasonal forecasts every month, for the
205 purpose of this study, we focus on the forecast initialized on November 1 (near the start of the
206 planting season) and January 1 (near the middle of the growing season) of 2015-16 event. Figure
207 2 shows the RZSM forecasts for the growing season made on November 1st of 2015. By this
208 time in the season, both FEWS NET and SADC had provided early warning of poor rainfall
209 performance in the region (Magadzire et al. 2017). The NHyFAS RZSM forecasts would have
210 provided further evidence of a looming unprecedented drought in the region. These forecasts
211 would have also indicated that RSA, which is the most important country for the region's food



212 production, was going to be within the epicenter of this drought event. These forecasts, in turn,
213 could potentially have triggered appropriate actions earlier by the early warning agencies as well
214 as the decision-makers (e.g., national governments and international relief agencies).

215 Later in the season as the observed precipitation data became available, RZSM
216 monitoring products would have provided refined estimates of the spatial extent and severity of
217 drought in the region. Figure 2 (bottom panel) shows the RZSM monitoring product available
218 after each of the months of November 2015 through February 2016. This monitoring product
219 would have provided additional proof of the drought occurrence in the region and shown that
220 RSA was within the epicenter of this drought. It is important to state that even the monitoring
221 product can be effectively used as a predictor of food insecurity events as they are available
222 before the typical start of the harvest season (in April) and the lean season (in November).

3.2 Performance of NHyFAS in supporting food insecurity early warning

223 Next, we investigate the long-term performance of NHyFAS in supporting food
224 insecurity early warning by examining how well forecasting and monitoring products available
225 from this system can explain historical variability in regional crop yield of the SA region and in
226 particular, help identify below-normal regional yield events. Regional crop yield is calculated by
227 adding the yearly productions from the SA countries, then dividing it by the yearly total
228 harvested area. The regional crop yield is then detrended to remove the effect of any long-term
229 changes (such as technological changes) on the regional yield.

230 For this analysis, we make use of the February RZSM forecasts initialized on November
231 1 and January 1, and February RZSM monitoring product (available in early March), as February
232 RZSM historically has the highest correlation with the detrended crop yield, as highlighted in



233 Fig. 3. This figure also indicates that February RZSM has higher correlation with detrended crop
234 yield than December-February (DJF) seasonal precipitation and air temperature however the
235 difference in correlation is not statistically significant.

236 Figure 4 (a & b) show the interannual covariability of February RZSM forecasts (based
237 on ESP method and bias-corrected GEOS forecasts) initialized on November 1 and January 1,
238 respectively, with the detrended regional crop yield. The correlation between GEOS-based
239 February RZSM forecasts initialized on November 1 is 0.49, which is higher than the correlation
240 based on monitoring products at this point in the season (Fig. 3). This indicates that a more
241 skillful (than the monitoring product) early warning of regional crop yield can be potentially
242 made as early as on November 1, about 4-5 months before the harvest season starts (around
243 April) and about a year before the next lean season (around November) starts. The correlation
244 value remains similar (0.45) even when the forecast is initialized on January 1; however, the
245 correlation value is still higher than what can be achieved using the monitoring product at this
246 point in the season (Fig. 3). Furthermore, the correlation values of GEOS-based RZSM forecasts
247 is higher than ESP-based RZSM forecasts. ESP-based RZSM forecasts derive their skill from the
248 initial hydrologic conditions only, whereas GEOS-based RZSM forecasts derive their skill from
249 the climate forecasts as well. Hence, the source of additional skill of GEOS-based RZSM
250 forecasts is the climate forecasts.

251 Figure 4 (c) shows the covariability of the February RZSM monitoring product with the
252 detrended regional yield. The correlation value with the regional crop yield increases to 0.79 and
253 is substantially higher relative to when RZSM forecasting products are used (Fig. 4a and b).
254 February RZSM monitoring product is available in early March, so a high correlation of the



255 regional crop yield with that product potentially means that early warning of regional crop yield
256 can be made with a high skill, about 1-2 months before the harvest season starts (around April)
257 and about 8-9 months before the next lean season (around the next November) starts. This is
258 likely to strengthen FEWS NET's current food insecurity early warning efforts in the region.

259 Next, we examine how well the forecasting and monitoring RZSM products do in
260 providing early warning of below-normal crop yield events. This criterion for performance
261 evaluation is of particular significance for food insecurity early warning in the region, as
262 below-normal crop yield events are the ones which generally lead to food insecurity. To
263 investigate this, we calculate the probability of below-normal crop yield events when either
264 February RZSM forecasting products (initialized on November 1 and January 1), and RZSM
265 monitoring product for the month of November (available in early December) through the month
266 of February (available in early March) were in the lower tercile. In this case, below-normal
267 regional crop yield events are the events that lie in the bottom 18 (i.e. bottom half) when
268 detrended crop yields for the 36 years is ranked in ascending order. Similarly, lower terciles of
269 RZSM products are the values that are in the bottom 12 (i.e. bottom tercile) of the RZSM
270 products when ranked in ascending order. In the case of RZSM, the ranked climatology is
271 different for each of the forecasting products and the monitoring products for each month.

272 Figure 5 shows the fraction of years with below-normal crop yield when February RZSM
273 forecasts (made on November 1 or January 1) were in the lower tercile (shown by blue color
274 bars) or when monthly RZSM monitoring products (shown by green color bars) were in the
275 lower tercile. These results indicate that as early as November 1, if the February RZSM is being
276 forecasted to be in the lower tercile, then there is about ~66% probability of the regional crop



277 yield being below normal (statistically significant at 86% confidence level). This would be 4-5
278 months before the start of the harvest season and about one year before the start of the next lean
279 season. The inferred probability value increases to ~83% when the February RZSM forecasts,
280 initialized in January, are in the lower tercile (statistically significant >95% confidence level).
281 Finally, by early March, by the time monitoring of February of RZSM is available, the inferred
282 probability increases to 100% (statistically significant >95% confidence level). In other words,
283 over 1982-2016, whenever the February RZSM for the SA region was in the lowest tercile, the
284 crop yield in the following season had been below normal (based on detrended yield). This
285 would be 1-2 months before the start of the harvest season and about 8-9 months before the start
286 of the next lean season.

287 Of course, the estimation of these probabilities is necessarily limited by the small sample
288 sizes examined; the actual probability of low crop yield based on low February RZSM, for
289 example, while apparently high, is not a full 100%. Nevertheless, these results provide, overall,
290 further evidence of the suitability of the forecasting and monitoring products from the NHyFAS
291 in supporting early warning of food insecurity in the region.

4 Discussion

292 This study makes a case for the application of NHyFAS's RZSM forecasting and
293 monitoring products in supporting the early warning of food insecurity in SA. It has been shown
294 that the successful early warning of crop yield, and especially below-normal crop yield years,
295 can be issued based on these products, which would offer significant implications for the region's
296 food security. Here, it is assumed that when the SA region faces a production shortfall, the
297 regional food insecurity is likely to rise. This was certainly the case during the 2015-16 El
298 Niño—which was the last major food insecurity event in the region. However, this narrow



299 assumption ignores other important factors that may lead to or further worsen food insecurity in
300 the region, such as inadequate agricultural inputs, price shocks (which can be global in nature),
301 rise in population, conflict, limited livelihood options, stocks, etc. Nonetheless, the direct
302 relationship of crop yield with the interannual variability in available moisture makes RZSM an
303 important variable for food security monitoring. It is of keen interest to early warning systems
304 like FEWS NET, which is presently the primary end user of the NHyFAS. Crop yield early
305 warning based on the NHyFAS products are also directly relevant to international collaborative
306 efforts like the GEOGLAM initiative and, particularly, to the Crop Monitor for Early Warning,
307 which provides monthly assessments of crop conditions for the countries most vulnerable to food
308 insecurity. Such assessments are key to helping reduce uncertainty of crop prospects as the
309 growing season progresses, and provide critical evidence for informing food security decisions
310 by humanitarian organizations and governments alike.

311 It is also worth mentioning here that crop yield reports can be influenced by external
312 factors (for example, reporting issues related to methods) other than long-term agricultural,
313 technology-driven changes and climate interannual variability. The effect of these factors on the
314 regional crop yield of course cannot be discounted by the detrending method employed in this
315 study.

316 Finally, the results of this study are also likely affected by the use of only one dynamical
317 climate forecast model for driving the seasonal hydrologic system. Adding forecasts from more
318 climate and hydrologic models would likely enhance the skill of the system. The choice of one
319 dynamical system was made mostly for operational purposes, since GEOS archived and



320 real-time forecasts include all atmospheric forcing variables needed to drive such LSMs, and are
321 available routinely to facilitate operational production of hydrologic forecasts.

5 Conclusions

322 The region of SA witnessed several food insecurity events in the last few decades.
323 Mitigation of food insecurity impact requires timely and effective interventions by national,
324 regional, and international agencies. To support those interventions, early warning of food
325 insecurity is needed. In this study, we investigate the suitability of the operational RZSM
326 products produced by a recently developed NASA seasonal scale hydrologic forecasting system,
327 NHyFAS, in supporting food insecurity early warning in this region.

328 The key findings of this study are: (i) the NHyFAS products would have identified the
329 regional severe 2015-2016 drought event (which peaked in December-February) at least as early
330 as November 1st of 2015; (ii) February RZSM forecasts produced as early as November 1 (4-5
331 months before the start of harvest, and about one year before the start of the next lean season)
332 can explain the interannual variability in regional crop yield production with moderate skill
333 (correlation 0.49); (iii) use of dynamical climate forecasts adds to the skill (relative to the skill
334 coming from the initial hydrologic conditions alone) of February RZSM forecasts in predicting
335 regional crop yield; (iv) the February RZSM monitoring product, available in early March (1-2
336 months before the start of harvest and 8-9 months before the start of the next lean season) can
337 explain the variability in regional crop yield with high skill (correlation of 0.79); (v) when the
338 February RZSM forecast (initialized on November 1) is found to be in the lowest tercile, the
339 subsequent detrended regional crop yield is below normal about 66% of the time (statistical
340 significance level ~86%), and likewise, when the February RZSM monitoring product is in the



341 lowest tercile, the subsequent crop yield, for the sampling period considered, is always
342 below-normal (statistical significance level >95%)

343 The NHyFAS products described here began being generated in August 2018 for
344 operational applications by FEWS NET. Each month, FEWS NET's regional scientists (located
345 in eastern, western and southern Africa) review the latest products ahead of the FEWS NET's
346 monthly climate discussions (Funk et al. 2019). The products are used to support or revise the
347 assumptions of climate and hydrologic conditions for the upcoming season. The updated
348 assumptions are then passed on to food analysts for the region in order to help inform needed
349 relief actions. The forecasting products are currently available via
350 <https://lis.gsfc.nasa.gov/projects/fame>.



Author contribution:

SS led the design of the analysis, conducted the analysis and wrote the manuscript and generated figures. KA, CL, CF and FD contributed to the design of the analysis. KA and AH conducted the model simulations. RK and CL reviewed the article and proposed substantial changes. CL and GH are PIs of projects supporting this work. TM, JV, AM, AH facilitate real-time application of the products. Rest of the co-authors reviewed the article and provided their input/edits.

Competing interests:

The authors declare that they have no conflict of interest.

Acknowledgements:

Support for this study comes from NASA Grant NNX15AL46G and the US Geological Survey (USGS) cooperative agreement #G09AC000001. Crop yield, production, and consumption data were obtained from USDA FAS's PSD:

<https://apps.fas.usda.gov/psdonline/app/index.html#/app/home>. Average price data were obtained

from FAO's FAO STATS database <http://www.fao.org/faostat/en/#home>. World Bank

Development Indicators were downloaded from <https://data.worldbank.org/indicator/>. GEOS

forecast data sets are generated and supported by NASA's Global Modeling and Assimilation

Office (GMAO). High-performance computing resources were provided by the NASA Center for

Climate Simulation (NCCS) in Greenbelt, MD. The authors thank Climate Hazards Center's

technical writer Juliet Way-Henthorne for providing professional editing.



References

- Archer, E., Landman, W. A., Tadross, M. A., Malherbe, J., Weepener, H., Maluleke, P. and Marumbwa, F. M.: Understanding the evolution of the 2014–2016 summer rainfall seasons in southern Africa: Key lessons, *Climate Risk Management*, 16, 22–28, 2017.
- Arsenault, K., Shukla, S., Hazra, A., Getirana, A., McNally, A., Kumar, S., Koster, R., Zaitchik, B., Badr, H., Jung, H. C., Narapusetty, B., Navari, M., Wang, S., Mocko, S., Funk, C., Harrison, L., Husak, G., Verdin, J. V., and Peters-Lidard, C. C.: A NASA modeling and remote-sensing based hydrological forecast system for food and water security applications. *Bulletin of the American Meteorological Society* (in review)
- Borovikov, A., Cullather, R., Kovach, R., Marshak, J., Vernieres, G., Vikhliaev, Y., Zhao, B. and Li, Z.: GEOS-5 seasonal forecast system, *Clim. Dyn.*, doi:10.1007/s00382-017-3835-2, 2017.
- Cane, M. A., Eshel, G. and Buckland, R. W.: Forecasting Zimbabwean maize yield using eastern equatorial Pacific sea surface temperature, *Nature*, 370(6486), 204–205, 1994.
- Csiszar, I. and Gutman, G.: Mapping global land surface albedo from NOAA AVHRR, *Journal of Geophysical Research: Atmospheres*, 104(D6), 6215–6228, doi:10.1029/1998jd200090, 1999.
- Diro, G. T.: Skill and economic benefits of dynamical downscaling of ECMWF ENSEMBLE seasonal forecast over southern Africa with RegCM4, *Int. J. Climatol.*, 36(2), 675–688, 2015.
- Ducharne, A., Koster, R. D., Suarez, M. J., Stieglitz, M. and Kumar, P.: A catchment-based approach to modeling land surface processes in a general circulation model: 2. Parameter estimation and model demonstration, *J. Geophys. Res. D: Atmos.*, 105(D20), 24823–24838, 2000.
- FAO, 2019: FAOSTAT Database. FAO. Rome, Italy. <http://www.fao.org/publications/en>
Accessed on July 1, 2019
- Friedl, M. A., McIver, D. K., Hodges, J. C. F., Zhang, X. Y., Muchoney, D., Strahler, A. H., Woodcock, C. E., Gopal, S., Schneider, A., Cooper, A., Baccini, A., Gao, F. and Schaaf, C.: Global land cover mapping from MODIS: algorithms and early results, *Remote Sensing of Environment*, 83(1-2), 287–302, doi:10.1016/s0034-4257(02)00078-0, 2002.
- Funk, C., Peterson, P., Landsfeld, M., Pedreros, D., Verdin, J., Shukla, S., Husak, G., Rowland, J., Harrison, L., Hoell, A. and Michaelsen, J.: The climate hazards infrared precipitation with stations—a new environmental record for monitoring extremes, *Sci Data*, 2, 150066, 2015.



Funk, C., Davenport, F., Harrison, L., Magadzire, T., Galu, G., Artan, G. A., Shukla, S., Korecha, D., Indeje, M., Pomposi, C., Macharia, D., Husak, G. and Nsadisa, F. D.: Anthropogenic Enhancement of Moderate-to-Strong El Niño Events Likely Contributed to Drought and Poor Harvests in Southern Africa During 2016, *Bull. Am. Meteorol. Soc.*, 99(1), S91–S96, 2018.

Funk, C., Shukla, S., Thiaw, W. M., Rowland, J., Hoell, A., McNally, A., Husak, G., Novella, N., Budde, M., Peters-Lidard, C., Adoum, A., Galu, G., Korecha, D., Magadzire, T., Rodriguez, M., Robjhon, M., Bekele, E., Arsenault, K., Peterson, P., Harrison, L., Fuhrman, S., Davenport, F., Landsfeld, M., Pedreros, D., Jacob, J. P., Reynolds, C., Becker-Reshef, I. and Verdin, J.: Recognizing the Famine Early Warning Systems Network (FEWS NET): Over 30 Years of Drought Early Warning Science Advances and Partnerships Promoting Global Food Security, *Bulletin of the American Meteorological Society*, doi:10.1175/bams-d-17-0233.1, 2019.

Gelaro, R., McCarty, W., Suárez, M. J., Todling, R., Molod, A., Takacs, L., Randles, C. A., Darmenov, A., Bosilovich, M. G., Reichle, R., Wargan, K., Coy, L., Cullather, R., Draper, C., Akella, S., Buchard, V., Conaty, A., Da Silva, A. M., Gu, W., Kim, G., Koster, R., Lucchesi, R., Merkova, D., Nielsen, J. E., Partyka, G., Pawson, S., Putman, W., Rienecker, M., Schubert, S. D., Sienkiewicz, M. and Zhao, A. B.: The Modern-Era Retrospective Analysis for Research and Applications, Version 2 (MERRA-2), *J. Climate*, 30, 5419–5454, 2017.

Guo, Z. and Dirmeyer, P. A.: Evaluation of the Second Global Soil Wetness Project soil moisture simulations: 1. Intermodel comparison, *Journal of Geophysical Research*, 111(D22), doi:10.1029/2006jd007233, 2006.

Gutman, G. and Ignatov, A.: The derivation of the green vegetation fraction from NOAA/AVHRR data for use in numerical weather prediction models, *International Journal of Remote Sensing*, 19(8), 1533–1543, doi:10.1080/014311698215333, 1998.

Hoell, A. and Cheng, L.: Austral summer Southern Africa precipitation extremes forced by the El Niño–Southern oscillation and the subtropical Indian Ocean dipole, *Clim. Dyn.*, 50(9–10), 3219–3236, 2017.

Hoell, A., Funk, C., Zinke, J. and Harrison, L.: Modulation of the Southern Africa precipitation response to the El Niño Southern Oscillation by the subtropical Indian Ocean Dipole, *Clim. Dyn.*, 48(7–8), 2529–2540, 2016.

Hoell, A., Gaughan, A. E., Shukla, S. and Magadzire, T.: The Hydrologic Effects of Synchronous El Niño–Southern Oscillation and Subtropical Indian Ocean Dipole Events over Southern Africa, *J. Hydrometeorol.*, 18(9), 2407–2424, 2017.

Koster, R. D., Suarez, M. J., Ducharne, A., Stieglitz, M. and Kumar, P.: A catchment-based approach to modeling land surface processes in a general circulation model: 1. Model structure, *J. Geophys. Res. D: Atmos.*, 105(D20), 24809–24822, 2000.



- Kumar, S., Peterslidard, C., Tian, Y., Houser, P., Geiger, J., Olden, S., Lighty, L., Eastman, J., Doty, B. and Dirmeyer, P.: Land information system: An interoperable framework for high resolution land surface modeling, *Environmental Modelling & Software*, 21(10), 1402–1415, 2006.
- Landman, W. A. and Beraki, A.: Multi-model forecast skill for mid-summer rainfall over southern Africa, *Int. J. Climatol.*, 32(2), 303–314, 2010.
- Landman, W. A. and Goddard, L.: Statistical Recalibration of GCM Forecasts over Southern Africa Using Model Output Statistics, *J. Clim.*, 15(15), 2038–2055, 2002.
- Landman, W. A., Mason, S. J., Tyson, P. D. and Tennant, W. J.: Retro-active skill of multi-tiered forecasts of summer rainfall over southern Africa, *Int. J. Climatol.*, 21(1), 1–19, 2001.
- Manatsa, D., Mushore, T. and Lenouo, A.: Improved predictability of droughts over southern Africa using the standardized precipitation evapotranspiration index and ENSO, *Theor. Appl. Climatol.*, 127(1-2), 259–274, 2015.
- Martin, R. V., Washington, R. and Downing, T. E.: Seasonal Maize Forecasting for South Africa and Zimbabwe Derived from an Agroclimatological Model, *J. Appl. Meteorol.*, 39(9), 1473–1479, 2000.
- Meque, A. and Abiodun, B. J.: Simulating the link between ENSO and summer drought in Southern Africa using regional climate models, *Clim. Dyn.*, 44(7-8), 1881–1900, 2014.
- Moody, E. G., King, M. D., Schaaf, C. B. and Platnick, S.: MODIS-Derived Spatially Complete Surface Albedo Products: Spatial and Temporal Pixel Distribution and Zonal Averages, *Journal of Applied Meteorology and Climatology*, 47(11), 2879–2894, doi:10.1175/2008jamc1795.1, 2008.
- Niu, G.-Y., Yang, Z.-L., Mitchell, K. E., Chen, F., Ek, M. B., Barlage, M., Kumar, A., Manning, K., Niyogi, D., Rosero, E., Tewari, M. and Xia, Y.: The community Noah land surface model with multiparameterization options (Noah-MP): 1. Model description and evaluation with local-scale measurements, *J. Geophys. Res.*, 116(D12), doi:10.1029/2010jd015139, 2011.
- Pomposi, C., Funk, C., Shukla, S., Harrison, L. and Magadzire, T.: Distinguishing southern Africa precipitation response by strength of El Niño events and implications for decision-making, *Environ. Res. Lett.*, 13(7), 074015, 2018.
- Reynolds, C. A., Jackson, T. J. and Rawls, W. J.: Estimating soil water-holding capacities by linking the Food and Agriculture Organization Soil map of the world with global pedon databases and continuous pedotransfer functions, *Water Resources Research*, 36(12), 3653–3662, doi:10.1029/2000wr900130, 2000.



SADC: SADC Regional Vulnerability Assessment and Analysis Synthesis Report 2016: State of Food Insecurity and Vulnerability in the Southern African Development Community : Compiled from the National Vulnerability Assessment Committee (NVAC) Reports Presented at the Regional Vulnerability Assessment and Analysis (RVAA) Annual Dissemination Forum on 6-10 June 2016 in Pretoria, Republic of South Africa., 2016.

Sheffield, J., Wood, E. F., Chaney, N., Guan, K., Sadri, S., Yuan, X., Olang, L., Amani, A., Ali, A., Demuth, S. and Ogallo, L.: A Drought Monitoring and Forecasting System for Sub-Sahara African Water Resources and Food Security, *Bull. Am. Meteorol. Soc.*, 95(6), 861–882, 2014.

Shukla, S., McNally, A., Husak, G. and Funk, C.: A seasonal agricultural drought forecast system for food-insecure regions of East Africa, *Hydrology and Earth System Sciences Discussions*, 11(3), 3049–3081, doi:10.5194/hessd-11-3049-2014, 2014.

Sunday, R. K. M., Masih, I., Werner, M. and van der Zaag, P.: Streamflow forecasting for operational water management in the Incomati River Basin, Southern Africa, *Physics and Chemistry of the Earth, Parts A/B/C*, 72-75, 1–12, 2014.

Trambauer, P., Werner, M., Winsemius, H. C., Maskey, S., Dutra, E. and Uhlenbrook, S.: Hydrological drought forecasting and skill assessment for the Limpopo River basin, southern Africa, *Hydrol. Earth Syst. Sci.*, 19(4), 1695–1711, 2015.

Verdin, K. L. and Verdin, J. P.: A topological system for delineation and codification of the Earth's river basins, *Journal of Hydrology*, 218(1-2), 1–12, doi:10.1016/s0022-1694(99)00011-6, 1999.

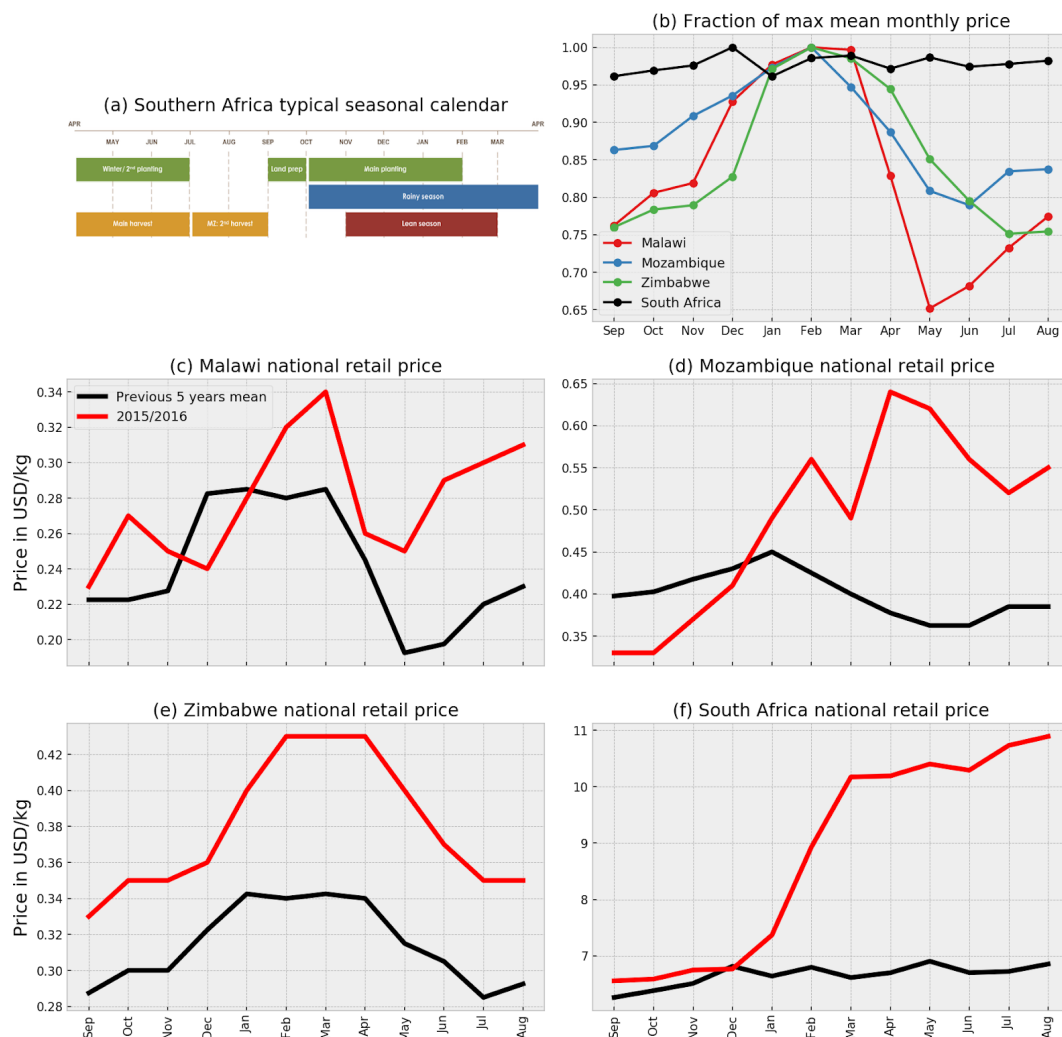
Winsemius, H. C., Dutra, E., Engelbrecht, F. A., Van Garderen, E. A., Wetterhall, F., Pappenberger, F. and Werner, M. G. F.: The potential value of seasonal forecasts in a changing climate in southern Africa, *Hydrol. Earth Syst. Sci.*, 18(4), 1525–1538, 2014.

Wood, A. W., Maurer, E. P. and Kumar, A., and Lettenmaier, D. P.: Long-range experimental hydrologic forecasting for the eastern United States, *J. Geophys. Res.*, 107(D20), doi:10.1029/2001jd000659, 2002.

Yang, Z.-L., Niu, G.-Y., Mitchell, K. E., Chen, F., Ek, M. B., Barlage, M., Longuevergne, L., Manning, K., Niyogi, D., Tewari, M. and Xia, Y.: The community Noah land surface model with multiparameterization options (Noah-MP): 2. Evaluation over global river basins, *J. Geophys. Res.*, 116(D12), doi:10.1029/2010jd015140, 2011.



352



353

354 **Figure 1: (a) Schematic representation of a typical seasonal calendar for the southern**
 355 **Africa region. (taken from: <http://fews.net/southern-africa>) (b) Monthly climatology of**
 356 **maize prices in SA countries. The monthly mean prices are normalized relative to the**
 357 **maximum mean monthly price for a given country, as the actual values of the mean**
 358 **monthly prices are different for different countries. Comparison of mean monthly maize**

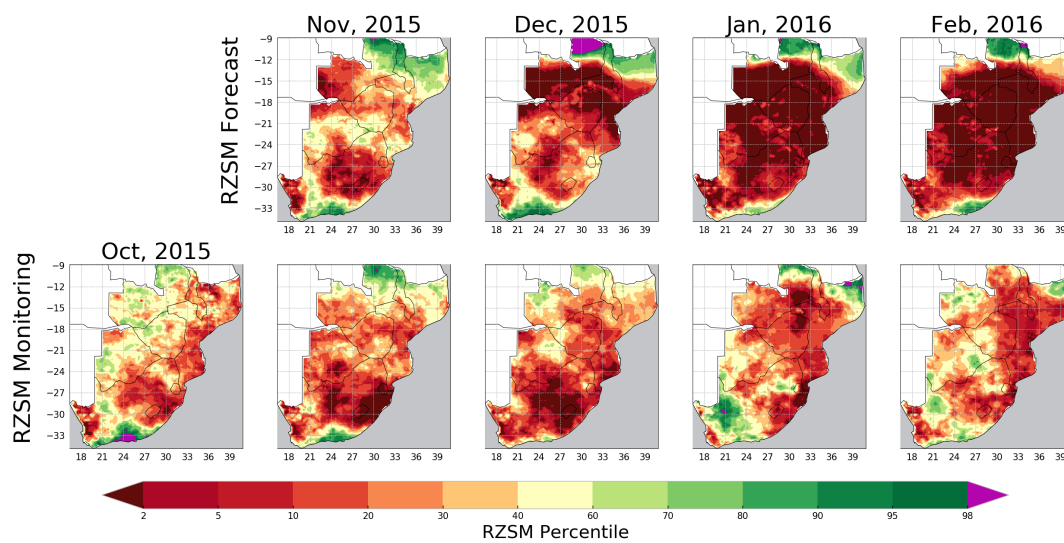


359 **prices for (c) Malawi (d) Mozambique (e) Zimbabwe (f) South Africa, during the 2015-16**
360 **event (red line) with the previous 5-year mean prices (black line). The price data is**
361 **available from FAOSTAT (FAO 2019).**



362

363



364

Figure 2: Forecast (top panel) and Monitoring of Rootzone soil moisture (RZSM)

365

percentiles for the months of November 2015 through February 2016. October 2015

366

conditions reflect forecast initialized on November 1, 2015. The RZSM monitoring

367

product for a given month is available during the early part of the following month. The

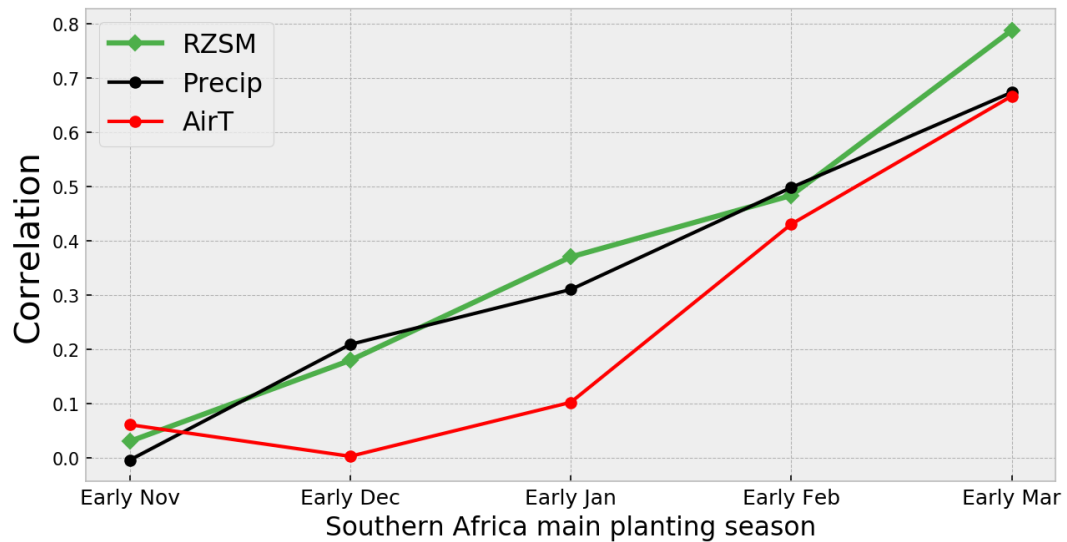
368

historical climatology (1982-2010) was used to calculate percentile.

369



370



371 **Figure 3: Variability of the correlation between the 3-month seasonal precipitation,**
372 **3-month seasonal air temperature (AirT), and monthly RZSM monitoring product with the**
373 **detrended crop yield. This result highlights that RZSM is potentially a better predictor of**
374 **crop yield than seasonal precipitation and AirT; also, the skill is the highest in early March**
375 **when DJF seasonal precipitation, AirT, and February RZSM monitoring products are**
376 **available.**

377

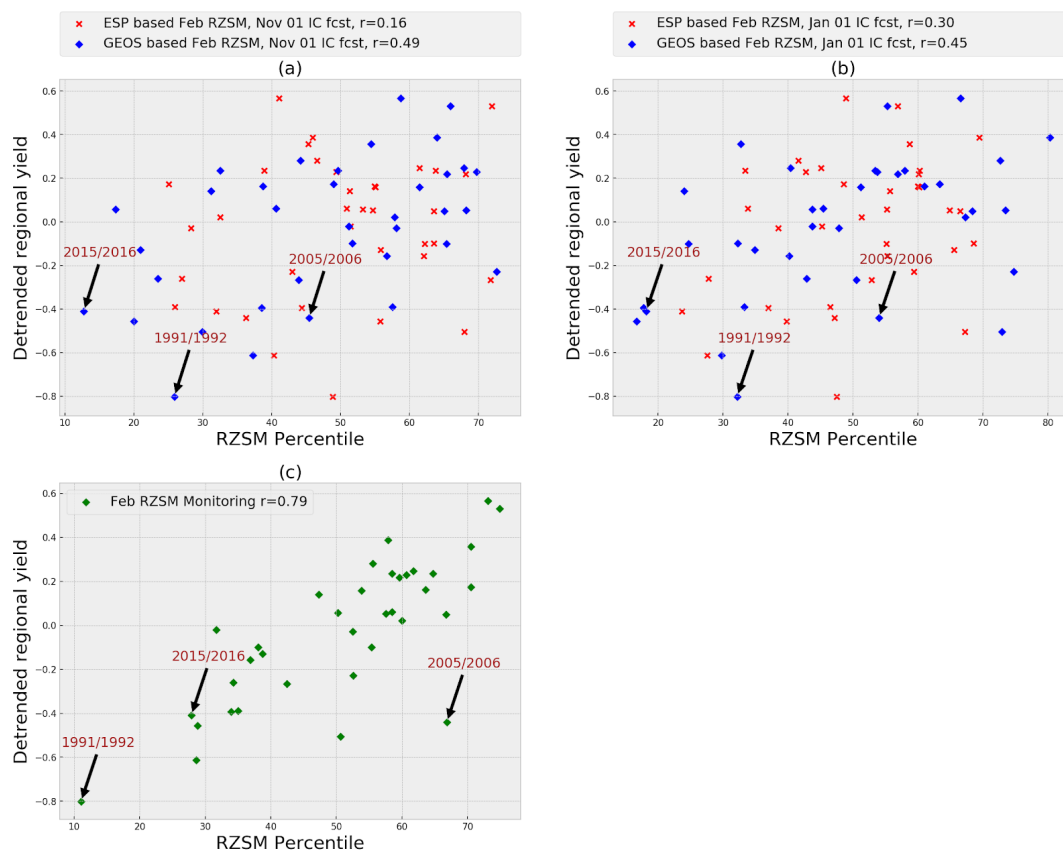


Figure 4: Covariability of (a) February RZSM forecasts (initialized on November 1) generated using ESP method and bias-corrected GEOS forecasts, (b) February RZSM forecasts (initialized on January 1) generated using ESP method and bias-corrected GEOS forecasts, and (c) the February RZSM monitoring product (available in early March), with detrended regional yield in southern Africa.

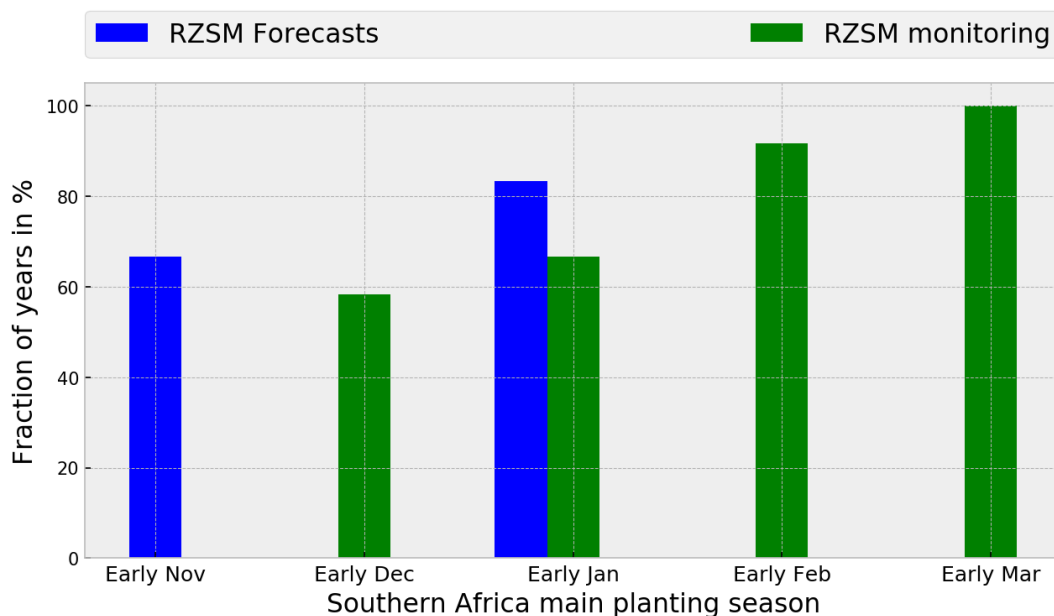


Figure 5: Fraction of years with below-normal regional crop yield (based on the rank of detrended crop yield) given that the corresponding RZSM forecasts (initialized on November 1 and January 1) and RZSM monitoring product (available in early March) were in the lowest tercile (based on the rank of the RZSM climatology). Note that the Nov 1 [Jan 1] RZSM forecasts-based probability of ~66% [~83%] is statistically significant at the ~86% [~95%] confidence level.